# Fast semi-analytic Sequential Explicit Coupling Analysis of 3D Planar Hydraulic fracturing

Luis Fernando Paullo Muñoz[1,2], Cristian Mejia[1], Julio Rueda[1], Deane Roehl[1,2]

[1]*Institute Tecgraf, Pontifical Catholic University of Rio de Janeiro*
*Rua Marquês de São Vicente 225 - Gávea, 22451-240, Rio de Janeiro, RJ, Brazil*
[2]*Civil and Environmental Engineering Department, Pontifical Catholic University of Rio de Janeiro*
*Rua Marquês de São Vicente 225 - Gávea, 22451-240, Rio de Janeiro, RJ, Brazil*
*lfernand@tecgraf.puc-rio.br, crisms@ tecgraf.puc-rio.br, julioa@tecgraf.puc-rio.br, deane@tecgraf.puc-rio.br*

**Abstract.** Hydraulic fracturing is a relevant issue in Geomechanics, especially when analyzing hydrocarbon production and associted physical phenomena. Several numerical, analytic, and semi-analytic methods have been developed to predict fluid-driven fracture propagation response. Traditional continuum-based numerical coupling methods, such as FEM or XFEM, allow the study of complex and realistic scenarios. However, they frequently require enormous computational effort, which is more evident in 3D modeling.On the other hand, most analytic solutions provide fast estimates but are limited to basic conditions, such as the analysis of the fracture domain only. In this context, semi-analytic methods are presented as an alternative that can provide solutions faster than traditional numerical methods. In addition, those methods apply to more realistic scenarios than analytic solutions. This work proposes a sequential explicit two-way coupling methodology to analyze planar hydraulic fracture propagation in pressurized rock formations. The coupling methodology associates the Finite Element Method used to solve the fluid flow problem with the semi-analytical Displacement Discontinuity Method to solve the mechanical problem. The proposed approach allows predicting fluid-driven fracture propagation in a planar domain considering arbitrary in-situ stresses and fluid flow conditions in the surrounding porous medium. The numerical results are compared to asymptotic analytical and numerical solutions, showing good accuracy and expressively lower computational cost than traditional numerical schemes.

**Keywords:** Hydraulic fracturing, Coupled analysis, DDM method, iterative scheme.

## 1 Introduction

Hydraulic fracturing is a relevant issue in Geomechanics, especially in assessing unconventional hydrocarbon reservoir production [1,2]. The fracturing process involves several complex physical phenomena, such as mechanical deformation, fluid migration, thermal state variation, and chemical reactions [3,4]. Among these phenomena, hydraulic and mechanical behaviors are significant in determining the response of hydraulic fracturing. These aspects have attracted the attention of multiple researchers aiming to study hydromechanical coupled participation [7,8,9].

Several numerical, analytic, and semi-analytic methods have been developed to predict fluid-driven fracture propagation response. Analytical methods, such as simplified KGD [10,11,12] or penny-shaped solutions [13,14], provide fast solutions for the evolution of hydraulic fracturing.Nevertheless, these solutions are generally limited to specific scenarios characterized by regular reservoir geometries, homogeneous media, regular fracture propagation shapes, etc. On the other hand, numerical methods such as Finite Element Methods (FEM) [15,16], Boundary Element Methods (BEM)[17,18], and Extended Finite Element Methods (X-FEM)[19,20], among others, allow the analyses of more complex and realistic problems, including arbitrary domain geometry, layered formations, and non-uniform fluid distribution. However, these numerical methods require robust computational capacity, especially in tridimensional problems where the number of unknowns reaches the order of millions. In this context, semi-analytical methodologies appear as attractive alternatives for solving problems involving realistic conditions while maintaining a low computational effort compared to more general numerical methods. In this sense, several researchers have utilized the Displacement Discontinuity Method (DDM), a boundary-based formulation developed by Crouch [21], to model the mechanical response of hydraulic fracturing propagation. Studies, ranging from two-dimensional fracturing simulations [22,23] to complex three-dimensional fracture propagation [24,] show the capability and flexibility of DDM in handling mechanical problems. However, DDM is frequently associated with hydraulic analysis, primarily focusing on fluid flow inside the fracture [25]. Paullo Muñoz et al. [26] proposed a coupling scheme combining FEM and DDM to assess two-dimensional hydraulic fracture propagation under fluid migration from the fracture to the surrounding media condition. The coupling strategy is another important aspect of the hydraulic fracturing analysis. Various fully coupled and pseudo-coupled schemes have been formulated to address fluid-driven fractures. Fully coupled formulations [27] offer more accurate results. However, they are computationally expensive. On the other hand, pseudo-coupled schemes provide faster solutions once the order of their resulting system of equations is considerably lower. Furthermore, purely sequential schemes [28] have been proposed to attain accurate results for pseudo-coupled solutions while maintaining reasonable computational efficiency. This work proposes a sequentially coupled 3D-DDM-FEM approach to study planar hydraulic fracturing in homogenous rock formations. Building upon the previous work by Paullo et al. [26], this approach extends the capabilities to three-dimensional scenarios. It employs an explicit two-way coupling scheme based on fracture aperture and fluid pore pressure. The numerical results exhibit excellent agreement compared to analytic solutions for penny-shaped hydraulic fractures.

# 2 Numerical formulations

## 2.1 Mechanical analysis

The displacement discontinuity method is adopted to evaluate mechanical behavior, which is based on establishing a discontinuity of the displacement field. For 3D planar fracture, the discontinuity is symmetric to the original plane in local coordinates, as shown in Figure 1, where the discontinuity amplitude $w$ represents the separation between the $C^+$ and $C^-$ planes.

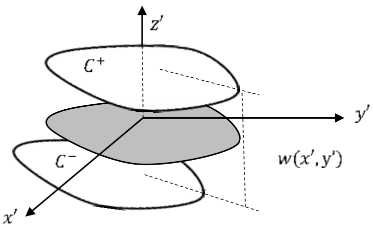


Figure 1. Schematic representation of a discontinuity in a continuum medium.

Navier's equations establish the mechanical equilibrium as follows,

$$\nabla^2 U_i = \frac{1}{1-2\nu} \sum_j \frac{\delta^2 U_i}{\delta x_i \delta x_j} = 0 \tag{1}$$

where U is the displacement field, $\nu$ is Poisson's coefficient, and $x_i$ indicates the $i^{th}$ cartesian direction. The solution for each particular case must consider the corresponding boundary conditions. The proposed approach adopts the following assumptions to solve the mechanical problem: homogenous medium, linear elastic material, and small strains and displacements (geometrically linear).

Defining a planar and rectangular discontinuity with dimensions $\Delta x$ and $\Delta y$ as shown in Figure 2, the normal discontinuity field $w$ can be expressed as:

$$w = A_z D(\xi, \eta) \ = u_z(\xi, \eta, 0+) - u_z(\xi, \eta, 0-) \tag{2}$$

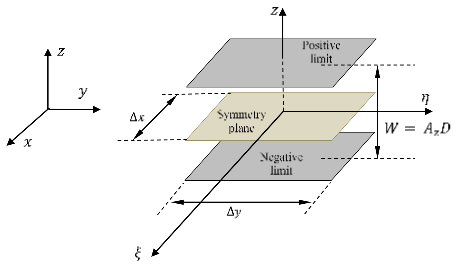


Figure 2. A rectangular planar portion of discontinuity in an infinite space.

where $\xi$ and $\eta$ are the discontinuity's local coordinates, $A_z$ is the amplitude, and $D(\xi, \eta)$ is a normalized discontinuity shape. The solution of equation (1) results in the following fundamental solution of the displacement field

$$\begin{aligned} Ux \ &= A_z(-(1-2\nu)I,_z - zI,_{xz}) \\ Uy \ &= A_z\left(-(1-2\nu)I,_y - zI,_{yz}\right) \\ Uz \ &= A_z(-(1-2\nu)I,_z - zI,_{zz}) \end{aligned} \tag{3}$$

where the kernel function $I$ is given by

$$I(x, y, z) = \frac{E}{8\pi(1-\nu)} \int \int_A \frac{D(\xi,\eta)}{[(x-\xi)^2+(y-\eta)^2+z^2]} \, d\xi d\eta \tag{4}$$

and $E$ is Young's modulus. The strain field can be derived by applying the linear kinematic relationship, and stresses can be obtained through the generalized Hooke law. For hydraulic fracturing, the component of interest is the normal stress, $\sigma_{zz}$, which is expressed as,

$$\sigma_{zz} \ = 2GA_z(f,_{zz} + zf,_{zzz}) \tag{5}$$

where $G = E/(1-2\nu)$ is the elastic shear modulus. Substituting equation (4) in (5), and Considering $D(\xi, \eta) = 1$ and planar propagation, i.e., z = 0 the normal stress component is given by

$$\sigma_{zz}(x, y) = -A_z \frac{E}{8\pi(1-\nu)} \left[ \left[ \frac{1}{[(x-\xi)^2+(y-\eta)^2]^{3/2}} \right]_{-\Delta x/2}^{\Delta x/2} \right]_{-\Delta y/2}^{\Delta y/2} \tag{6}$$

The amplitude of the displacement discontinuity field can be obtained by establishing known boundary conditions to ensure stress equilibrium inside the fracture. For this, the fracture domain is discretized into a finite number of rectangular displacement discontinuity elements. Hydraulic fracturing is established by the equilibrium of normal stresses within each element considering the in-situ far stress field and the internal fluid pressure. Thus, the following system of equations can be formulated,

$$p_i + \sigma_{0,i} = \sum_{j=1}^{N} C_{i,j} A_{z_j} \qquad i = 1..N \tag{7}$$

where $p$ is the internal fluid pressure, $\sigma_0$ represents the far normal stress, and $C_{i,j}$ is the coefficient of deformability contribution obtained from equation (5) for three-dimensional cases. Equation (7) can be expressed in matrix form as

$$\boldsymbol{H} \, \bar{A} = \overline{\boldsymbol{\sigma}} \tag{8}$$

where $\boldsymbol{H}$ represents the stiffness matrix that is symmetric and positive definite. The numerical procedure proposed is similar to that adopted for two-dimensional cases [26].

### 2.2 Hydraulic Analysis

The hydraulic analysis follows using Finite Element Methods. The governing equation for isothermal single-phase flow in porous media, assuming Darcy flow without compositional effects, is given by

$$\frac{1}{M}\frac{\partial p}{\partial t} + \nabla \boldsymbol{v} = Q \tag{9}$$

where $p$ represents the fluid pore pressure, $\boldsymbol{v}$ is the fluid seepage velocity, $Q$ is the fluid source and/or sink, $\nabla$ is the gradient operator, and $M$ is Biot's modulus. The seepage velocity is expressed as

$$\boldsymbol{v} = \boldsymbol{k}_m \left\{\frac{\nabla p}{\gamma_f} - \boldsymbol{i}_g\right\} \tag{10}$$

where $\boldsymbol{k}_m$ is the hydraulic conductivity matrix, $\boldsymbol{i}_g$ is the gravity vector, and $\gamma_f$ is the specific fluid weight. The continuity equation, Eq. (9), can be discretized using the standard Galerkin method, which results in

$$\frac{1}{M}\int_{\Omega} \boldsymbol{N}_p^T \boldsymbol{N}_p d\Omega.\dot{\boldsymbol{p}} + \int_{\Omega} \boldsymbol{B}_p^T \frac{\boldsymbol{k}_m}{\gamma_f} \boldsymbol{B}_p d\Omega. p = \int_{\Gamma} Q\, \boldsymbol{N}_p d\Gamma \tag{11}$$

where $\boldsymbol{B}_p = \begin{bmatrix} \frac{\partial \boldsymbol{N}_p}{\partial x} & \frac{\partial \boldsymbol{N}_p}{\partial y} \end{bmatrix}$, $\boldsymbol{p}$ is the nodal pore fluid pressure, and $\boldsymbol{N}_p$ is the shape function vector.

Reynold's lubrication theory governs fluid flow inside the fracture channel, which occurs in the longitudinal direction inside the fracture and the normal direction at the top and bottom fracture surfaces. Assuming Newtonian, isothermal, and incompressible fluid, Equation (9) can be rewritten as

$$\frac{\partial q_f}{\partial x} + q_T + q_B = q_i \tag{12}$$

where $q_f$ is the longitudinal fluid flow, $q_i$ is the fluid injected into the fracture channel, $q_T$ and $q_B$ are the fluid leak through the top and bottom faces of the fracture into the porous medium, respectively. The cubic law of parallel plates governs the longitudinal fluid flow $q_f$ inside the fracture that depends on the fracture aperture $\Delta_n$ and is defined as,

$$q_f = -\frac{\Delta_n^3}{12.u_f}\frac{\partial p_f}{\partial x} \tag{13}$$

here $u_f$ is the fluid viscosity and $p_f$ is the fluid pressure inside the fracture. According to the continuum case, the continuity equation in the fractures Eq. (12) can be discretized using the standard Galerkin method. More details of the hydraulic formulation used in this work can be found in [14].

### 2.3 Coupling parameters

The discontinuity amplitude assessed through the DDM formulation determines the fracture aperture of the interface elements used in the hydraulic FEM analysis. Consequently, it becomes feasible to establish a coupling relationship involving fracture aperture, pore pressure, and the stress field inside the fracture, as defined by:

$$\bar{\sigma}_i \approx p_i^* + \sigma_{0,i}, \quad \Delta_n^* \approx A_{z_i} \tag{14}$$

where $p_i^*$ is the internal fluid pressure at the center of the interface element and $\Delta_n^*$ represents the fracture aperture. All numerical processes are performed in an in-house framework Gema [29]. The explicit two-way coupled scheme with fixed time increments implemented in Paullo Muñoz et al. [26] is adopted here.

# 3 Numerical Examples

## 3.1 Penny Shaped: Impermeable case

The first benchmark consists of a penny-shaped hydraulic fracture in an impermeable homogeneous porous medium. The results of the proposed DDM-FEM approach are compared against those obtained via a penny-shaped analytic solution presented by Gao and Ghassemi [30]. Figure 3 depicts a prismatic domain discretized by regular hexahedral elements. The horizontal region where the fracture surface is expected is discretized by squared interface-DDM elements with a square size equal to L=0.20m. In the impermeable case, mesh discretization in the vertical direction is irrelevant to the response since fluid flow is confined to the horizontal fracture surface (interface elements). Figure 3 also shows the hydromechanical properties of the problem.

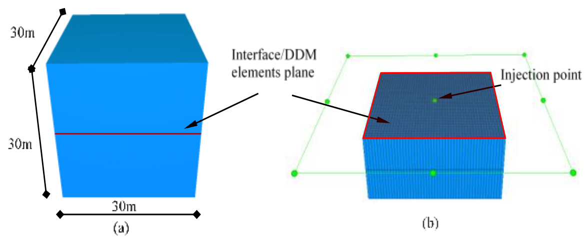


| Properties | Symbol | Values | Units |
|---|---|---|---|
| Young's modulus | $E$ | 38.8 | $GPa$ |
| Poisson's ratio | $\nu$ | 0.15 | --- |
| Fracture toughness | $K_{IC}$ | 8.91 | $MPa.m^{0.5}$ |
| Tensile strength | $\tau_c$ | 14.0 | $MPa$ |
| Hydraulic conductivity | K | $10^{-16}$ | m/s |
| Fluid specific weight | $\gamma_f$ | 9.8 | kPa/m |
| Biot coefficient | $B$ | 1.0 | -- |
| Dynamic fluid viscosity | $\mu$ | 0.0005 | $Pa.s$ |
| Injection flow rate | $Q_0$ | 0.001 | $m^3/s$ |

Figure 3. 3D DDM-FEM model with regular mesh.

Figure 4 shows the pressure evolution at the injection point over time, considering the variation of the time increment dt. As expected, the comparison between the proposed approach and analytical solution shows convergence with the reduction of dt, validating the implementation of the proposed methodology for this case of study.

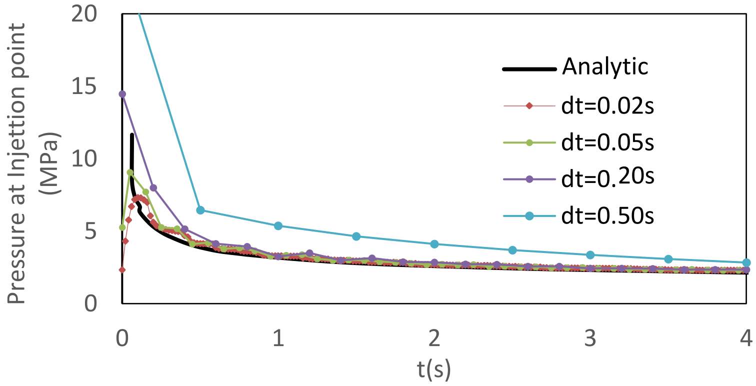


Figure 4. Pressure vs time at injection point.

## 3.2 Penny-shaped fracture: near M-Vertex regime

The second benchmark evaluates the capability of the proposed methodology to predict penny-shaped fracture propagation under the viscosity-dominated regime, commonly referred to as the M-Vertex regime [15]. This example employs the same model as the previous example, i.e., with L = 0.20 m. The time increment adopted for this example is dt = 0.1s. The numerical results are compared with the analytical solution presented by Zielonka et al. [16]. The hydromechanical properties adopted in [16] are summarized in Table 1.

Table 1. Hydromechanical properties for the penny-shaped problem under M-vertex regime [19]

| Properties | Symbol | Values | Units |
|---|---|---|---|
| Young's modulus | $E$ | 20 | $GPa$ |
| Poisson's ratio | $\nu$ | 0.25 | --- |
| Fracture toughness | $K_{IC}$ | 1.0 | $MPa.m^{0.5}$ |
| Tensile strength | $\tau_c$ | 1.0 | $MPa$ |
| Hydraulic conductivity | $K$ | $9.8 \times 10^{-9}$ | m/s |
| Fluid specific weight | $\gamma_f$ | 9.8 | kPa/m |
| Biot coefficient | $B$ | 0.75 | -- |
| Dynamic fluid viscosity | $\mu$ | 0.001 | $Pa.s$ |
| Injection flow rate | $Q_0$ | 0.001 | $m^3/s$ |

Figure 5 shows the evolution of the fracture aperture and the pressure at the injection point obtained with the proposed DDM-FEM scheme and the analytic solution presented in [16] over time. The proposed solution shows good agreement with the analytic solution for the fracture aperture and injection pressure when comparing with other numerical methods (see [16]). These results show that the proposed methodology can predict the hydraulic fracture propagation in problems with fluid migration into the rock formations.

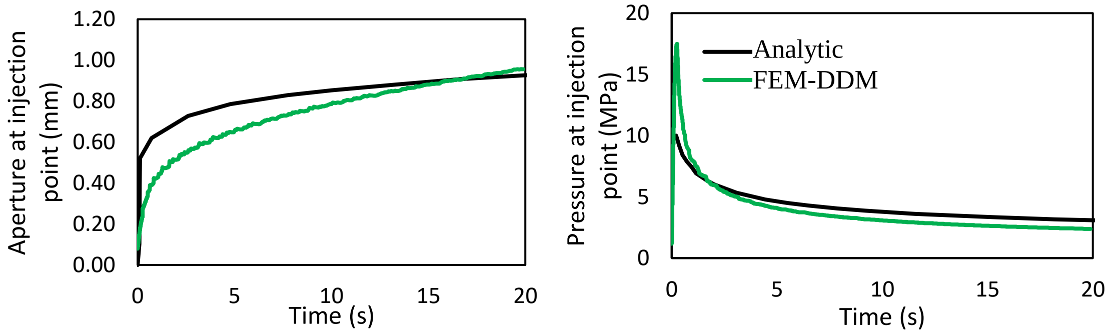


Figure 5. Fracture aperture and pressure vs time at injection point.

## 4 Conclusions

This work proposes an explicit coupling scheme that combines the Finite Element Method (FEM) for fluid migration and the Displacement Discontinuity Method (DDM) for mechanical analysis. Numerical results concerning the penny-shaped problem under impermeable conditions demonstrate that reducing the time increment contributes to the convergence of the FEM-DDM method towards the analytical solution. The results of the proposed methodlogy show no stability issues. The results of the proposed method closely align with the analytical solution when investigating penny-shaped fracture propagation under the M-Vertex regime. Results obtained with the proposed FEM-DDM coupling scheme exhibit good agreement with those obtained via the analytic solutions, underscoring the consistency of the proposed scheme.

**Acknowledgements**. The authors gratefully acknowledge the support from Brazilian National Council for Scientific and Technological Development (CNPq) Grant 315077/2023-9 and 308056/2022-1, Carlos Chagas Filho Foundation for Supporting research in the State of Rio de Janeiro (FAPERJ) Grants E-26/202.928/2019 and E-26/201.391/2021

**Authorship statement**. The authors hereby confirm that they are the sole liable persons responsible for the authorship of this work, and that all material that has been herein included as part of the present paper is either the property (and authorship) of the authors, or has the permission of the owners to be included here.

## References

[1] Economides, M.J., Nolte, K.G., 2013. Reservior Stimulation, vol. 18 Wiley, New York. https://doi.org/10.1017/CBO9781107415324.004.
[2] Hu, G., Phan, H., Ouache, R. Gandhi, H., Hewage, K., Sadiq R., 2019. Fuzzy fault tree analysis of hydraulic fracturing flow back water storage failure. Journal of Natural Gas Science and Engineering, 72, 103039.
[3] Li, Q., Xing, H., Liu, J., Liu, X., 2015. A review on hydraulic fracturing of unconventional reservoir. Petroleum 1 (1), 8–15. https://doi.org/10.1016/j.petlm.2015.03.008.
[4] Anderson, T.L. Fracture Mechanics: Fundamentals and Applications: Fundamentals and Applications, Third Edition. Taylor and Francis. Ed. 2005.
[7] Zheltov A.K., 1955. Formation of vertical fractures by means of highly viscous liquid. 4th world pet congr,. p. 8.
[8] Sneddon, I.N. The distribution of stress in the neighbourhood of a crack in an elastic solid. Proc R Soc A Math Phys Eng Sci 1946;187:229–60. https://doi.org/10.1098/rspa.1946.0077.
[9] Ribeiro, P.M., Horne, R.N., 2013. Pressure and temperature transient analysis: hydraulic fractured well Application. In: Society of Petroleum Engineers (Ed.), SPE Annual Technical Conference and Exhibition. Society of Petroleum Engineers (SPE). https://doi.org/10.2118/166222-ms.
[10] Geertsma J, De Klerk F., 1969. A rapid method of predicting width and extent of hydraulically induced fractures. J Pet Technol, 21:1571–81. https://doi.org/10.2118/2458-PA.
[11] Simonson, E.R., Abou-Sayed, A.S., Clifton, R.J., 1978. Containment of massive hydraulic fractures. Soc. Pet. Eng. J. 18 (1), 27–32.
[12] Fung, R.L., Vijayakumar, S., Cormack, D.E., 1987. Calculation of Vertical Fracture Containment in Layered Formations. SPE Form.4:1(35).
[13] Detournay, E., 2004. Propagation regimes of fluid-driven fractures in impermeable rocks. Int. J. Geomech. 4 (1), 35–45. https://doi.org/10.1061/(ASCE)1532-3641(2004).
[14] Bunger, A. P., Detournay, E., Garagash, D. I., 2005. “Toughness-Dominated Hydraulic Fracture with Leak-Off,” International Journal of Fracture, 134, pp.175-190.
[15] Carrier, B., Granet, S., 2012. Numerical modeling of hydraulic fracture problem inpermeable medium using cohesive zone model. Eng. Fract. Mech. 79, 312–328. https://doi.org/10.1016/j.engfracmech.2011.11.012
[16] Zielonka MG, Searles KH, Ning J, Buechler SR., 2014. Development and validation of fullycoupled hydraulic fracturing simulation capabilities. SIMULIA community conf. SCC2014. p. 1–31.
[17] Dahi Taleghani A, Gonzalez-Chavez M, Yu H, Asala H., 2018. Numerical simulation of hydraulic fracture propagation in naturally fractured formations using the cohesive zone model. J Pet Sci Eng, 165:42–57. https://doi.org/10.1016/j.petrol.2018.01.063.
[18] Rueda, J., Mejia, C., Roehl, D., 2019. Hydromechanical modeling of unrestricted crack propagation in fractured formations using intrinsic cohesive zone model. Comput. Geotech. 221, 290–300. https://doi.org/10.1016/j.engfracmech.2019.106655
[19] Cruz, F., Roehl, D., Vargas, E. , 2018. An XFEM element to model intersections between hydraulic and natural fractures in porous rocks. International Journal of Rock Mechanics and Mining Sciences 2018, 112, 385-397.
[20] Gutiérrez, R., Mejia, C., Roehl, D., Romanel, C. 2019. Xfem modeling of stress shadowing in multiple hydraulic fractures in multilayered formations. Journal of Natural Gas Science and Engineering 70 (2019) 102950.
[21] Crouch SL., 1976. Solution of plane elasticity problems by the displacement discontinuity method. I. Infinite body solution. Int J Numer Meth Engng, 10, 301–43.
[22] Dong C, De Pater C., 2001. Numerical implementation of displacement discontinuity method and its application in hydraulic fracturing. Comput Methods Appl Mech Engng, 191:745–60.
[23] Chen, E. Leung, C., Tang, S., Lu, C., 2018. Displacement discontinuity method for cohesive crack Propagation. Engineering Fracture Mechanics, 190, 319–330.
[32] Abass, H.H., Brumley, J.L., Venditto, J.J., 1994. Oriented perforations – A rock mechanics view. SPE Annu Tech Conf Exhib.
[24] Huiying Tang a, Shihao Wang b, Ruihan Zhang a, Sanbai Li c, Liehui Zhang a, Yu-Shu Wu b,2019. Analysis of stress interference among multiple hydraulic fractures using a fully three-dimensional displacement discontinuity method, Journal of Petroleum Science and Engineering, 179, -378-393.
[25] Ming Chen a,b, Shicheng Zhang a, Sihai Li a,c, Xinfang Ma a, Xi Zhang c, Yushi Zou. 2020. An explicit algorithm for modeling planar 3D hydraulic fracture growth based on a super-time-stepping method. International Journal of Solids and Structures, 191-192, 370-389.
[26] Paullo Muñoz L.F., Mejia, C., Rueda J., Roehl, D. 2022. Pseudo-coupled hydraulic fracturing analysis with displacement discontinuity and finite element methods. Engineering Fracture Mechanics. 274, article 108774.
[27] Rueda, J., Mejia, C., Roehl, D., 2019. Hydromechanical modeling of unrestricted crack propagation in fractured formations using intrinsic cohesive zone model. Comput. Geotech. 221, 290–300. https://doi.org/10.1016/j.engfracmech.2019.106655
[28] R. Quevedo, D. Roehl. A novel and efficient sequential-explicit technique for poroelasticity problems. Computer and Geotechnics, 138 (2021), https://doi.org/10.1016/j.compgeo.2021.104334
[29] Mendes, C.A.T., 2016. GeMA, um novo framework para a prototipação, desenvolvimento e integração de simulações multifísicas e multiescalas em grupos multidisciplinares, in Departamento de Informática. Pontifícia Universidade Católica do Rio de Janeiro: Rio de Janeiro. p. 168.
[30] Qian Gao, Ahmad Ghassemi, 2020. Three dimensional finite element simulations of hydraulic fracture height growth in layered formations using a coupled hydromechanical model. Int. J. Rock Mec. & Mining Sc, 125, article 104137.